Optical and structural properties of III-V nitrides under pressure

N.E. Christensen
Institute of Physics and Astronomy, Aarhus University, DK-8000 Aarhus C, Denmark

I. Gorczyca
High Pressure Research Center "Unipress," Polish Academy of Sciences, 01-142 Warsaw, Poland
(Received 3 February 1994; revised manuscript received 21 April 1994)

Self-consistent linear muffin-tin-orbital band-structure calculations are used to investigate the optical and structural properties of III-V semiconducting nitrides under hydrostatic pressure. The pressure behavior of the energy band structures is discussed in the context of the postulated chemical trends in III-V semiconductors. The regions in **k** space of dominant interband contributions to the elements of structure in the dielectric functions are identified. The total-energy calculations suggest that all the nitrides under pressure transform to the semiconducting rocksalt phase. The calculated transition pressures are 21.6 GPa (InN), 51.8 GPa (GaN), 16.6 GPa (AlN), and 850 GPa (BN). Experimental values that agree well with this have been found for the first three compounds. The fact that GaN and AlN have such different transition pressures in spite of their very similar ionicities is explained by the presence of 3*d* states on Ga.

I. INTRODUCTION

The aim of this paper is to examine the physical properties of the III-V nitrides, GaN, AlN, InN, and BN, with emphasis on their dependence on hydrostatic pressure. The nitrides form a specific subgroup of the III-V compounds characterized by high ionicity, very short bond lengths, low compressibility, and high thermal conductivity. These properties make them interesting and very useful. The III-V nitrides may, for example, find application in blue-light-emitting diodes and lasers operating in the blue and ultraviolet regime. They may also become important materials in high temperature diodes and transistors. Since the properties of electronic devices based on large-gap II-VI semiconductors tend to degrade with time, more and more attention is paid to the III-V nitrides. This is related to the fact that the formation energy of defects in these materials is very high.

Many physical properties of semiconductors can be scaled with material parameters such as atomic volume and ionicity. The theory proposed by Van Vechten[1] was based on this, and gave a qualitatively good classification of a large number of tetrahedrally coordinated semiconductors. The analysis also includes pressure effects. It is particularly interesting to investigate the pressure behavior of the nitrides, which are the most ionic semiconductors in the III-V group and have a very small atomic volume. By means of experiments and first-principles calculations it is possible to examine, over a wider parameter range, the chemical trends in the family of III-V compounds as deduced from models. The nitrides are therefore also interesting to basic research.

We study here the optical and structural properties of the III-V nitrides by means of band-structure and total-energy calculations performed for different volumes and crystal structures. The calculations were made by means of the linear muffin-tin-orbital (LMTO) method[2] in its scalar-relativistic form in conjunction with the local density approximation (LDA) to the density-functional theory. In the following sections the results of the calculations are presented and compared with experimental data. In Sec. II the pressure dependence of the energy band structure is presented and discussed in the context of chemical trends. In Sec. III the band structures obtained for different pressures are used to evaluate the imaginary part of the dielectric function under pressure. This function is directly related to the electronic band structure and thus allows investigations of the effects of external perturbations. A comparison with experimental data is made. The high pressure phases are investigated and discussed in Sec. IV. A summary of our results and conclusions is given in Sec. V, which also contains further discussions of the results. In particular, we there elaborate on the role of the Ga 3*d* states in connection with the pressure-induced structural transition.

II. PRESSURE DEPENDENCE OF BAND STRUCTURES

The band structures of the III-V nitrides for several crystal structures were calculated by means of the LMTO method in its scalar-relativistic form,[2] in conjunction with the local density approximation (LDA). Here we applied the simplest version of the LMTO method, the atomic-sphere approximation,(ASA)[2] but the "combined correction" terms[2] were incorporated. The details of the LDA-LMTO calculations for zinc-blende-type semiconductors are given elsewhere.[3,4] The wurtzite structure, in which GaN, AlN, and InN crystallize at ambient conditions, is somewhat more complicated for this kind of calculation. The unit cell contains four "real" atoms and four so-called "empty spheres."[3,4] The calculations were optimized by the choice of equal atomic-sphere radii for real atoms and different values for two types of empty

spheres.[5] Earlier calculations[6–8] of the electronic structure of GaAs, band offsets in semiconductor heterostructures, and structural properties of tin under pressure, have demonstrated the effects of including the "semicore" d states as fully relaxed band states. Based on this experience we found it necessary also in the present work to include the Ga $3d$ and In $4d$ states as band states. This is especially important for GaN, and we shall later (see the discussion in Sec. V) discuss in more detail how the Ga $3d$ states influence the pressure at which the $B3 \rightarrow B1$ transition occurs. The calculations for wurtzite structures were performed under the assumption that the crystal structure was "ideal," meaning that the c/a ratio was taken as equal to 1.633 and the internal bond-length parameter u was 3/8. Experimental c/a values are 1.627, 1.600, and 1.612 for GaN, AlN, and InN, respectively.[9] X-ray diffraction measurements[10] have shown that u=0.377 for GaN and 0.3821 for AlN. A detailed structural optimization was made earlier[11] for AlN, and the structural parameters obtained, c/a=1.596, u=0.3820, agree very well with the experimental values. The u parameter has, to our knowledge, not yet been determined for InN, but a theoretical value, u=0.380, was obtained by Yeh, Lu,

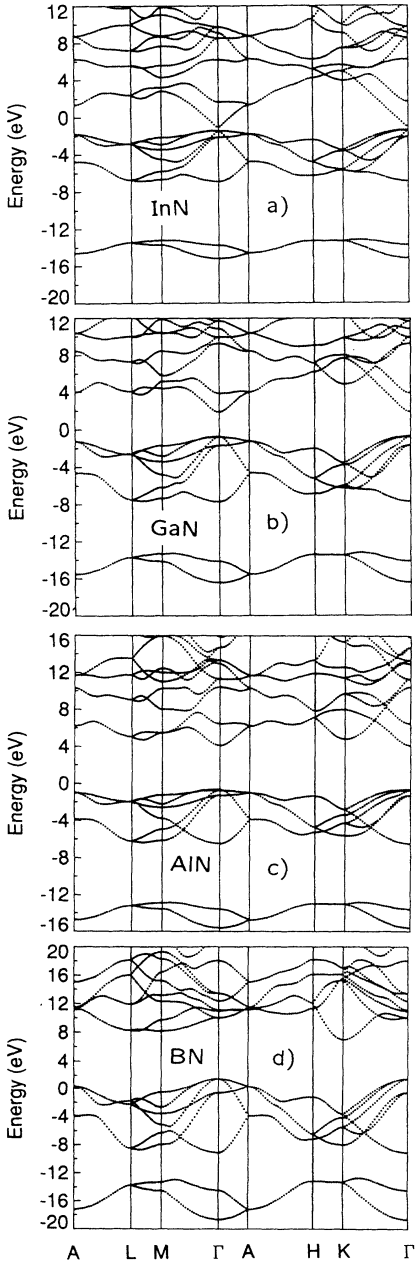

FIG. 1. Band structures for InN (a), GaN (b), AlN(c), and BN (d) in the wurtzite structure. (The Ga $3d$ and In $4d$ are included neither in this nor in the subsequent band-structure plots.)

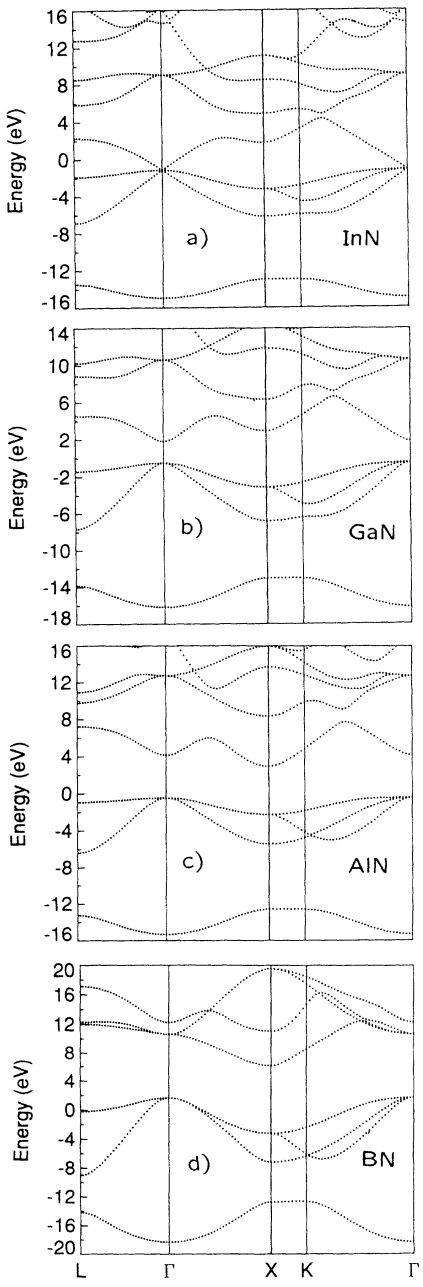

FIG. 2. Band structures for InN (a), GaN (b), AlN (c), and BN (d) in the zinc-blende structure.

Froyen, and Zunger.[12]

The LDA energy band structures of the nitrides for three crystal structures, wurtzite, zinc-blende, and rocksalt, are shown in Figs. 1–4. For the rocksalt phase we include results corresponding to two different volumes, one being the (theoretical) equilibrium volume, the other being the volume at the transition pressure. The latter volume is also as derived from the calculations (for InN, GaN, and AlN the wurtzite→rocksalt, and for BN the zinc-blende→rocksalt transition). The calculated band gaps as well as their deformation potentials are summarized in Tables I–III. Tables IV–VI below contain the coefficients for first- and second-order gap variations with lattice constant and pressure.

Since the semiconductor band gaps derived from LDA eigenvalues are too small, we performed, for InN, GaN, and AlN, additional calculations where the gaps were adjusted by inclusion of some external potentials.[3] These results are listed in the column headed by "adjusted." It should be noted, however, that the experimental data available are not sufficiently detailed to allow an accurate determination of the parameters of the adjusting poten-

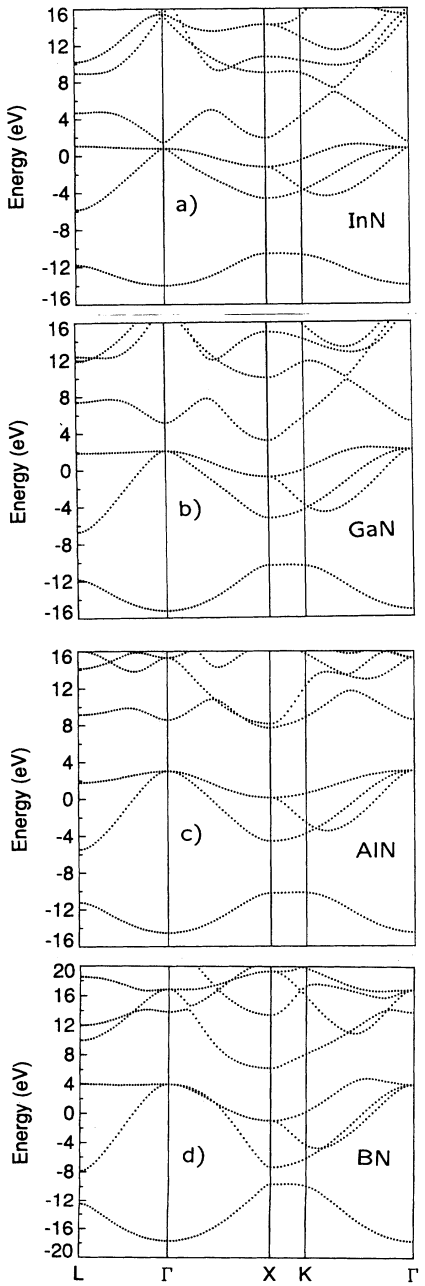

FIG. 3. Band structures for InN (a), GaN (b), AlN (c), and BN (d) in the rocksalt structure for the equilibrium lattice constant.

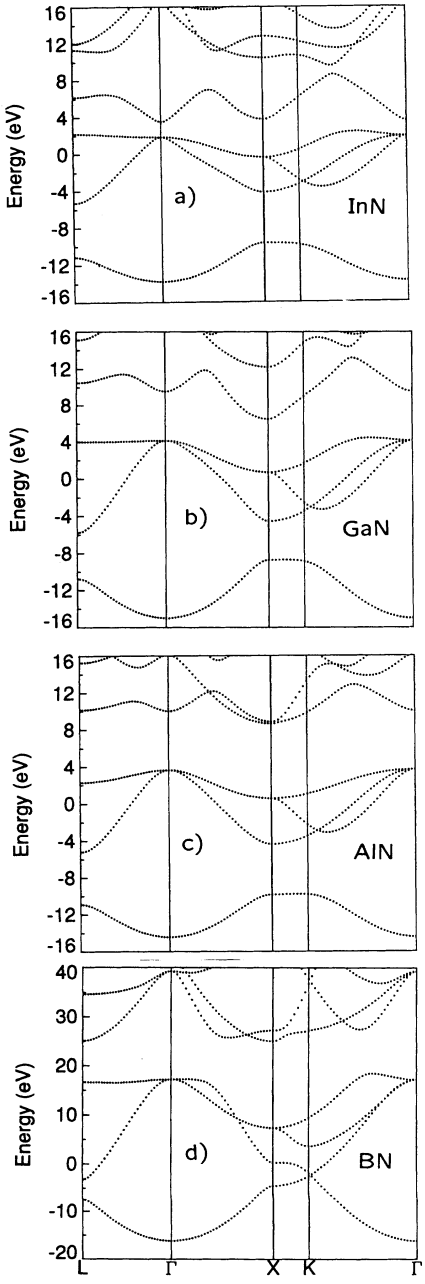

FIG. 4. Band structures for InN (a), GaN (b), AlN (c), and BN (d) in the rocksalt structure for the lattice constant at which the phase transition to the rocksalt structure occurs.

tials. Thus, although the minimum gaps are brought close to experiments, the dispersion of the present adjusted band structures may not predict future experiments very well. Our discussion of the nitride band structures and the optical properties will therefore mainly be made in terms of the LDA-eigenvalue bands.

Although the gaps are too small, their pressure coefficients are usually considered to be well described within

TABLE I. Energy gaps in eV and deformation potentials a of the nitrides in the wurtzite structure. Our calculated gaps are given for two volumes, V_{expt} and V_{th}, the experimental and theoretical equilibrium volumes, respectively. "Other results" includes experiments as well as theory. (The gap value [2.34] given to GaN is discussed in the text.)

	Gaps (eV)					a (eV)	
	Present work			Other calculations	Experiment	Present work	Other results
	LDA		adjusted				
InN	V_{expt}	V_{th}					
Γ_v-Γ_c	0.26	0.43	2.04	2.04,[a] 1.02,[b] 0.30(2.05)[c]	1.90,[d] 2.05,[e] 2.2[f]	-4.1	-3.3[f]
Γ_v-K_c	5.25	5.26	5.72	5.41(7.16)[c]		-0.23	
Γ_v-M_c	4.09	4.34	5.33	4.18(5.93)[c]		-5.4	
Γ_v-A_c	2.62	2.81	3.85			-4.1	
Γ_v-L_c	3.66	3.79	4.70			-2.8	
Γ_v-H_c	5.42	5.66	6.77			-5.1	
GaN							
Γ_v-Γ_c	2.45 [2.34]	2.64	3.44	3.0,[a] 2.71,[b] 2.42(3.65)[c] 1.63,[g] 2.76,[h] 3.0[i]	3.50,[j] 3.60,[k] 3.457 [l]	-7.8	-11.5[l]
Γ_v-K_c	5.45	5.44	6.35	5.74(6.97),[c] 4.57,[g] 4.93[h]		0.36	
Γ_v-M_c	5.09	5.17	5.94	5.22(6.45),[c] 4.63,[g] 5.02[h]		-2.8	
Γ_v-A_c	4.59	4.77	5.31	4.28,[g] 5.00[h]		-7.2	
Γ_v-L_c	4.67	4.75	5.49	3.99,[g] 4.54[h]		-3.4	
Γ_v-H_c	6.73	6.85	7.47	6.62[h]		-3.2	
AlN							
Γ_v-Γ_c	4.73	4.78	6.05	4.64,[b] 4.56(6.28)[c] 3.09,[g] 4.4[m]	6.28[n]	-8.8	-7.1[g]
Γ_v-K_c	5.44	5.44	6.29	5.58(7.30),[c] 4.36[g]		-0.6	1.2[g]
Γ_v-M_c	6.10	6.11	6.82	5.90(7.62),[c] 4.93[g]		-2.8	-1.5[g]
Γ_v-A_c	6.83	6.88	7.78	5.57[g]		-8.8	-7.0[g]
Γ_v-L_c	5.69	5.71	6.60	4.59[g]		-3.4	-1.6[g]
Γ_v-H_c	7.80	7.81	8.56	7.14[g]		-3.5	-1.6[g]
BN							
Γ_v-Γ_c	8.50	8.52		8.0, [g] 8.89(11.0)[c]		-4.3	
Γ_v-U_c	6.72	6.72		5.81[b]		-3.7	
Γ_v-K_c	5.45	5.44		5.70(7.8)[c]		1.4	
Γ_v-M_c	6.66	6.67		6.65(8.7)[c]		-3.7	
Γ_v-A_c	9.63	9.66				-9.8	
Γ_v-L_c	6.75	6.76				-3.8	
Γ_v-H_c	9.84	9.86				-8.0	

[a]Model pseudopotential (Ref. 13).
[b]OLCAO (Ref. 14).
[c]LMTO; values in parentheses, include band-gap correction (Ref. 15).
[d]Absorption at 300 K (Ref. 16).
[e]Absorption at 300 K (Ref. 17).
[f]P. Perlin, preliminary result, which requires further confirmation.
[g]Nonlocal pseudopotential (Ref. 18).
[h]Norm conserving pseudopotential (Ref. 19).
[i]Norm conserving pseudopotential (Ref. 20).
[j]Photoluminescence excitation spectra (Ref. 21).
[k]Reflectivity (Ref. 22).
[l]Absorption at 20 K (Ref. 23).
[m]LCAO (Ref. 24).
[n]Absorption at 300 K (Ref. 25).

the LDA. This statement reflects experience obtained from calculations on several compound semiconductors, e.g., as in Ref. 36, and is further supported by theory.[37,38] A very recent calculation by Palummo *et al.*[29] of gap corrections using the *GW* method for cubic GaN indicates that the LDA gap in that case is too small by ≈0.97 eV. The same work also estimates the correction to the deformation potential (which is one-third of their[29] linear coefficient a_1) of the minimum gap at Γ. Within the LDA the deformation potential a is found[29] to be −6.95 eV, in good agreement with our value −7.4 eV (Table II). Inclusion of the *GW* correction yields $a = -8.96$ eV. This may indicate that some precaution should be taken when it is assumed in general that LDA errors do not show up in the gap deformation potentials.

The gap values, 2.34 eV and 2.03 eV, given in square brackets for GaN (Tables I and II) were obtained from a calculation that uses the same potentials as the other calculations, but where coupling to the low-lying (Ga 3*d*) as well as to the high-lying (Ga 4*d*) *d* states were simultaneously taken into account. Gaps given without brackets were GaN and InN two-panel calculations obtained directly from the upper-panel calculation, i.e., where the coupling is to the higher *d*'s only. (All two-panel calculations for GaN and InN do of course treat the low-lying *d* states as relaxed band states, and their major influence on the potential is thus taken into account.)

It follows that for GaN we find that the gap in the wurtzite structure exceeds the value of the zinc-blende phase by 2.34−2.03= 0.31 eV. This is slightly overestimated because the band structure of wurtzite GaN was calculated for the ideal structure. In the case of AlN

TABLE II. Energy gaps in eV and deformation potentials a of the nitrides in the zinc-blende structure. Our calculated gaps are given for two volumes, V_{expt} and V_{th}, the experimental and theoretical equilibrium volumes, respectively. V_{expt} was taken to be the same as in the wurtzite structure. "Other results" includes experiments as well as theory. (The gap value [2.03] given to GaN is discussed in the text.)

	Gaps (eV)				a (eV)	
	Present work		Other calculations	Experiment	Present work	Other results
	V_{expt}	V_{th}				
InN						
Γ_v-Γ_c	0.02	0.08	-0.09(1.66)[a]		-2.2	
Γ_v-L_c	3.28	3.41	3.37(5.12)[a]		-5.4	
Γ_v-X_c	2.87	2.87	2.85(4.60)[a]		-0.12	
GaN						
Γ_v-Γ_c	2.18	2.23	2.01(3.24),[a] 1.48[b]	3.52,[f] 3.2[g]	-7.4	-6.95,[h] -8.96[i]
	[2.03]		2.08,[c] 2.65,[d] 2.00[e]			
Γ_v-L_c	4.93	4.99	4.81(6.04)[a]		-7.7	
Γ_v-X_c	3.36	3.36	3.34(4.57)[a]		-0.05	
AlN						
Γ_v-Γ_c	4.58	4.53	4.52(6.0)[a]		-9.0	
Γ_v-L_c	7.69	7.64	7.65(9.15)[a]		-9.4	
Γ_v-X_c	3.39	3.40	3.36(4.9)[a]		-0.37	
BN						
Γ_v-Γ_c	8.92	8.93	8.84(11.0),[a] 8.6,[j,k] 8.7[l]		-4.9	
Γ_v-L_c	10.29	10.33	10.21(12.3)[a]		-11.0	
Γ_v-X_c	4.42	4.42	4.30(6.4),[a] 4.2,[j]	6.0,[m] 6.4[n]	-1.1	-1.6[j]
			8.5,[k] 5.18[l]	6.1[o]		

[a] LMTO; values in parentheses include band-gap correction (Ref. 15).
[b] Nonlocal pseudopotential (Ref. 18).
[c] Norm conserving pseudopotential (Ref. 20).
[d] Norm conserving pseudopotential (Ref. 19).
[e] Full potential LMTO (Ref. 26).
[f] Cathodoluminescence at 53 K on epitaxial films (Ref. 27).
[g] Absorption (Ref. 28).
[h] Pseudopotentials, LDA (Ref. 29).
[i] Pseudopotentials + *GW* (Ref. 29).
[j] Nonlocal pseudopotential (Ref. 30).
[k] Pseudopotential with nonlocal exchange potential (Ref. 31).
[l] OLCAO (Ref. 14).
[m] Emission spectra (Ref. 32).
[n] Ultraviolet absorption (Ref. 33).
[o] Vacuum ultraviolet absorption (Ref. 34).

TABLE III. The calculated energy gaps E_g of nitrides in the rocksalt structure for the equilibrium volume V_{eq} and for that one at which the phase transition occurs, V_T, and the corresponding deformation potentials a in comparison with other calculations and experimental data ("Other results" includes both experiment and theory).

	Gaps (eV)			a (eV)		
	Present work		Other calculations	Present work		Other results
	V_{eq}	V_T	V_{eq}	V_{eq}	V_T	V_{eq}
InN						
Γ_v-Γ_c	0.62	1.66		-9.2	-10.3	
Γ_v-L_c	3.91	4.35		-3.9	-4.3	
Γ_v-X_c	1.09	1.87		-7.0	-7.7	
Σ_v-Γ_c	0.21	1.17		-8.5	-9.5	
GaN						
Γ_v-Γ_c	2.92	5.26	3.16,[a]2.5[b]	-12.9	-15.6	
Γ_v-L_c	5.31	6.28		-5.6	-6.1	
Γ_v-X_c	1.00	2.29	1.01,[a]0.5[b]	-7.2	-8.3	
Σ_v-X_c	0.76	1.99		-6.8	-7.9	
AlN						
Γ_v-Γ_c	5.56	6.39	4.99[a]	-13.2	-14.9	-13.6[a]
Γ_v-L_c	6.13	6.50	5.52[a]	-5.9	-6.6	-5.4[a]
Γ_v-X_c	4.65	5.00	4.04[a]	-5.8	2.3	-7.5[a]
BN						
Γ_v-Γ_c	9.92	21.7		-19.3	-16.1	
Γ_v-L_c	5.92	7.74		-2.6	-2.3	
Γ_v-X_c	2.23	7.91		-7.4	4.1	
Σ_v-X_c	1.55	7.13		-7.2	4.4	

[a]Nonlocal pseudopotential (Ref. 18).
[b]Norm conserving pseudopotential (Ref. 35).

we found[11] that changing c/a and u from the ideal values to those resulting from a total-energy optimization (close to the observed values) causes a reduction of the wurtzite-AlN gap at Γ by 0.21 eV. Using, for GaN, the experimental structural parameters given above leads to a gap that is only 0.03 eV below the one obtained for the ideal structure. This smaller shift reflects the fact that for GaN the actual structure is closer to the ideal than is the case for AlN. In InN the structural relaxation reduces the gap at Γ by 0.06 eV. When reading Table I, it should be borne in mind that structural relaxations may change the gaps by amounts that are typically of the order of one-half to two-tenths of an eV. Thus, our best LDA gap at Γ for AlN is not the 4.73 eV given in Table I, but rather 4.52 eV. Also the gap deformation potentials are somewhat affected by structural relaxation. For AlN we found,[11] for the gap at Γ, $a = -9.1$ eV if the structure is assumed to be ideal (Table I lists -8.8 eV, a value that is slightly different due to technical details), but changing the atomic coordinates to their optimized values we obtained $a = -7.6$ eV. In the cubic structures there are, of course, no corrections to be made for structure relaxations.

The pressure behavior of the energy gaps has in general a sublinear character (Tables IV–VI). The values of the deformation potentials for the wurtzite and zinc-blende structures vary usually between -3 and -10 eV. Only for the Γ_v-K_c gaps in the wurtzite and the Γ_v-X_c gaps in the zinc-blende structure is a weaker, and almost linear, pressure dependence found. These gaps have deformation potentials which are small in magnitude. The deformation potentials in the rocksalt phase are large in magnitude, approaching the value of 19.3 eV for BN at the Γ point. The variation of the energy gap with pressure, as calculated here and measured by Perlin *et al.*,[39] is shown in Fig. 5 for GaN in the wurtzite structure. For the conventional III-V compounds the value of the pressure coefficient of the direct gap at the Γ point varies from 100 to 150 meV/GPa. For all the nitrides these coefficients are much smaller, ranging from 11 to 40 meV/GPa. This contradicts the empirical rule formulated by Paul[40] that pressure coefficients of electronic band-to-band transitions should be the same for all III-V compounds. Rather, it appears that the lattice constant as well as the ionicity should be taken into account in a description of the trends. We find that dE_g/dP increases with the lattice constant and decreases with ionicity. This behavior is illustrated in Fig. 6, where we present the pressure coefficients for the III-V compounds as a function of the ratio of lattice constant and ionicity. The ionicities were estimated by Van Vechten[1] and the values for the nitrides are somewhat higher (0.4–0.6) than typical values for other III-V semiconductors (0.2–0.3). Our ionicity values were obtained as in Ref. 42. The results, together with calculated and experimental lattice constants are summarized in Table VII. The ionicities calculated here are higher than those obtained by Van Vechten and much higher than ionicities of other III-

TABLE IV. The coefficients α, β, γ, and δ for the nitrides in the wurtzite structure related to $E = E(a_0) + \alpha(\Delta a/a_0) + \beta(\Delta a/a_0)^2$ and $E = E(0) + \gamma P + \delta P^2$, E being the relevant gap and a_0 the equilibrium lattice constant.

	α (eV)	β (eV)	γ (meV/GPa)	δ (meV/GPa^2)
InN				
Γ_v-Γ_c	-12	49	33	-0.55
Γ_v-K_c	-0.63	-11	1.9	-0.08
Γ_v-M_c	-16	-44	43	-1.1
Γ_v-A_c	-12	15	33	-0.87
Γ_v-L_c	-8.5	-6.5	23	-0.70
Γ_v-H_c	-15	-49	41	-1.6
GaN				
Γ_v-Γ_c	-23	23	39	-0.32
Γ_v-K_c	1.1	-16	-1.8	-0.03
Γ_v-M_c	-8.3	-6.9	14	-0.17
Γ_v-A_c	-21	25	36	-0.30
Γ_v-L_c	-10	-7.6	17	-0.21
Γ_v-H_c	-10	-30	16	-0.16
AlN				
Γ_v-Γ_c	-27	33	40	-0.32
Γ_v-K_c	-1.8	-10	2.7	-0.05
Γ_v-M_c	-8.0	-29	13	-0.24
Γ_v-A_c	-26	28	40	-0.33
Γ_v-L_c	-10	-3.8	16	-0.17
Γ_v-H_c	-11	-2.4	16	-0.17
BN				
Γ_v-Γ_c	-13	3.0	11	-0.05
Γ_v-K_c	4.1	-30	-3.5	-0.00
Γ_v-M_c	-11	-0.6	9.4	-0.04
Γ_v-A_c	-29	-45	25	-0.12
Γ_v-L_c	-11	-7.8	9.7	-0.03
Γ_v-H_c	-24	-18	21	-0.06

TABLE V. The coefficients α, β, γ, and δ for the nitrides in the zinc-blende structure related to $E = E(a_0) + \alpha(\Delta a/a_0) + \beta(\Delta/a_0)^2$ and $E = E(0) + \gamma P + \delta P^2$, E being the relevant gap and a_0 the equilibrium lattice constant.

	α (eV)	β (eV)	γ (meV/GPa)	δ (meV/GPa^2)
InN				
Γ_v-Γ_c	-6.6	42	16	-0.02
Γ_v-L_c	-16	21	40	-0.36
Γ_v-X_c	-0.37	-3.1	0.91	-0.02
GaN				
Γ_v-Γ_c	-22	22	40	-0.38
Γ_v-L_c	-23	30	42	-0.38
Γ_v-X_c	-0.14	-8.0	0.28	-0.03
AlN				
Γ_v-Γ_c	-27	37	42	-0.34
Γ_v-L_c	-28	31	44	-0.38
Γ_v-X_c	-1.1	-7.3	1.7	-0.03
BN				
Γ_v-Γ_c	-15	14	13	-0.03
Γ_v-L_c	-33	10	29	-0.32
Γ_v-X_c	-3.2	-3.2	2.8	-0.02

TABLE VI. The coefficients α, β, γ, and δ for the nitrides in the rocksalt structure related to $E = E(a_T) + \alpha(\Delta a/a_T) + \beta(\Delta a/a_T)^2$ and $E = E(P_T) + \gamma(P - P_T) + \delta(P - P_T)^2$, E being the relevant gap, a_T the lattice constant at the transition point, and P_T the transition pressure.

	α (eV)	β (eV)	γ (meV/GPa)	δ (meV/GPa^2)
InN				
Γ_v-Γ_c	-31	55	41	-0.08
Γ_v-L_c	-13	10	17	-0.10
Γ_v-X_c	-23	42	31	-0.00
Σ_v-Γ_c	-29	35	38	-0.12
GaN				
Γ_v-Γ_c	-46	74	39	-0.32
Γ_v-L_c	-18	23	15	-0.16
Γ_v-X_c	-25	39	21	-0.18
Σ_v-X_c	-24	38	20	-0.17
AlN				
Γ_v-Γ_c	-45	91	43	-0.18
Γ_v-L_c	-20	27	19	-0.09
Γ_v-X_c	6.9	150	-6.6	0.19
BN				
Γ_v-Γ_c	-48	62	5.9	-0.01
Γ_v-L_c	-7.0	-3.6	0.85	-0.00
Γ_v-X_c	12	29	-1.5	0.01
Σ_v-X_c	13	32	-1.6	0.01

V compounds. They are rather typical for II-VI semiconducting materials. Our values are very close to the ionicities g derived by Garciá and Cohen.[41]

III. DIELECTRIC FUNCTIONS

The complex dielectric functions $\varepsilon_2(\omega)$ for III-V nitrides were calculated and the assignment of the critical points to the band-structure energy differences at various points of the Brillouin zone was made in comparison with

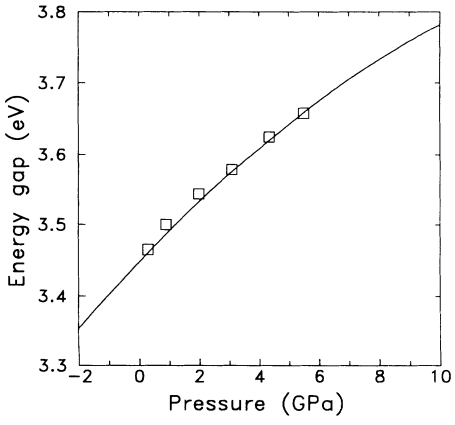

FIG. 5. Pressure dependence of the GaN energy gap showing the typical sublinear character. Solid line: our LDA calculations, but rigidly upshifted by ≈ 0.82 eV. The squares represent experimental results (Ref. 39).

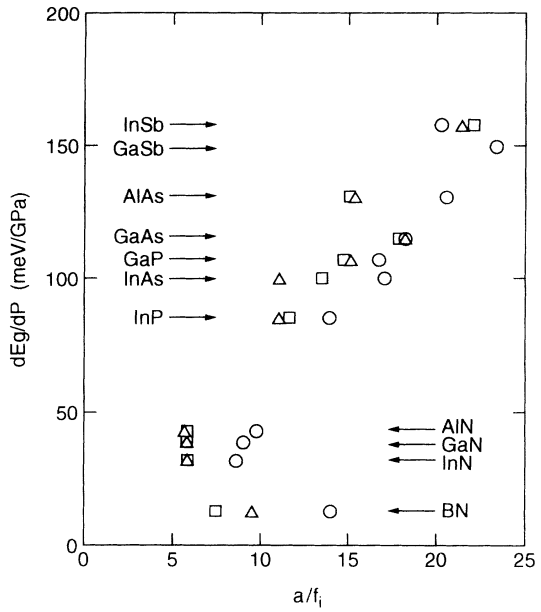

FIG. 6. Pressure coefficients of the direct gap of various III-V compounds as a function of the ratio between their lattice constant and ionicity f_i. Three sets of ionicities were used: Phillips ionicity (circles), ionicity values (g) as calculated by Garciá and Cohen (Ref. 41) (open squares), and our calculated ionicities (triangles).

some existing data. The Brillouin zones of the wurtzite and zinc-blende lattices, with the points of high symmetry indicated, are shown in Fig. 7. The calculated imaginary parts of the dielectric functions for photon energy up to 20 eV are shown in Figs. 8–11 below. For the wurtzite structure the dielectric functions are resolved into two components, $\varepsilon_{2xy}(\omega)$ which is the average of the spectra for polarizations along the x and the y directions, and $\varepsilon_{2z}(\omega)$ which corresponds to the polarization vector being parallel to the z direction (c axis). The averaged function $\varepsilon_2(\omega)= (\varepsilon_{2x} + \varepsilon_{2y} + \varepsilon_{2z})/3$ is also included. In Tables VIII–XI below the calculated critical-point energy gaps as well as more extended regions giving the dominant contributions to elements of structure in the dielectric functions are given. For some compounds (InN,BN) comparison with experimental data and other calculations is made. Below, the more detailed discussion of optical spectra is presented.

Considering the calculations one should bear in mind that they employ LDA one-particle band structures (too small gaps), and local-field effects[43,44] are not included. Further, we use here the atomic-sphere approximation (ASA), and this implies that the choice of the sphere radius ratio affects the amplitudes of the calculated spectra somewhat. Our method of extracting the dielectric functions is discussed in more detail elsewhere.[45–47]

A. InN

The characteristics of the major elements of structure in the $\varepsilon_2(\omega)$ spectrum as calculated from direct interband transitions in (wurtzite) InN are given in Table VIII. Figure 8 shows the ε_2 spectra calculated for the wurtzite (two polarizations and averaged) and for the zinc-blende structure. An assignment is suggested of structure elements found from experiment.[48] Also, the Table VIII enables a comparison to the pseudopotential calculations by Foley and Tansley.[49] The experimental imaginary part of the dielectric function was obtained from reflectance spectra of single-crystalline InN by the Kramers-Kronig analysis. The two spectra (our calculated and the experimental) are presented in Fig. 8(c). The intensity of the theoretical peaks is much higher than of those in the experimental trace. This is a general feature of all theoretical spectra derived in the single-particle scheme.[50] The calculated $\varepsilon_2(\omega)$ function begins with an M_0-type transition at Γ, corresponding to the main energy gap. Our calculated onset energy (0.26 eV, Table I) is much smaller than the experimental gap (2.2 eV) due to the LDA. The shoulder at 3.75 eV corresponds to the one at 4.0 eV in the experimental spectrum and to the one near 4 eV obtained from the pseudopotential calculations. The identification is the same, mainly Γ_{5v}-Γ_{3c} (using the labeling of transitions given in Ref. 49, i.e., numbering bands from below in energy, 4,5→10 transitions at Γ). The main peak is divided into two components at 4.61 and 4.73 eV, and experimentally it is found at 5 eV photon energy. The pseudopotential calculations give the values 4.8 eV and 5.1 eV with assignment to transitions at the Γ point (Γ_{5v}-Γ_{6c}, Γ_{5v}-Γ_{3c}) (see Fig. 4 of Ref. 49). A more detailed study of possible transitions and their matrix elements indicates that these two peaks originate in the region near a Σ point close to Γ and are due to transitions from band 4 to 10. So the second peak is indeed close to Γ_{5v}-Γ_{3c}. Next, there are two peaks (5.26 and 5.63 eV) with obvious counterparts in the experimental spectrum. A small feature in the pseudopotential calculations at 5.6 eV assigned to the U point is probably what we find as a shoulder at 5.85 eV, but which we assign to

TABLE VII. The calculated and experimental lattice constants and ionicities. For wurtzite structures we give the effective cubic lattice constant defined through $a_{\text{eff}}^3 = \sqrt{3}\,a^2c$. The Phillips ionicity values are from Ref. 1.

	Lattice constant (Å)		Ionicity		
	Present work	Experiment	Present work	Ref. 41	Phillips
InN	4.92	4.98	0.859	0.853	0.578
GaN	4.43	4.50	0.770	0.778	0.500
AlN	4.36	4.37	0.775	0.754	0.449
BN	3.62	3.61	0.380	0.484	0.256

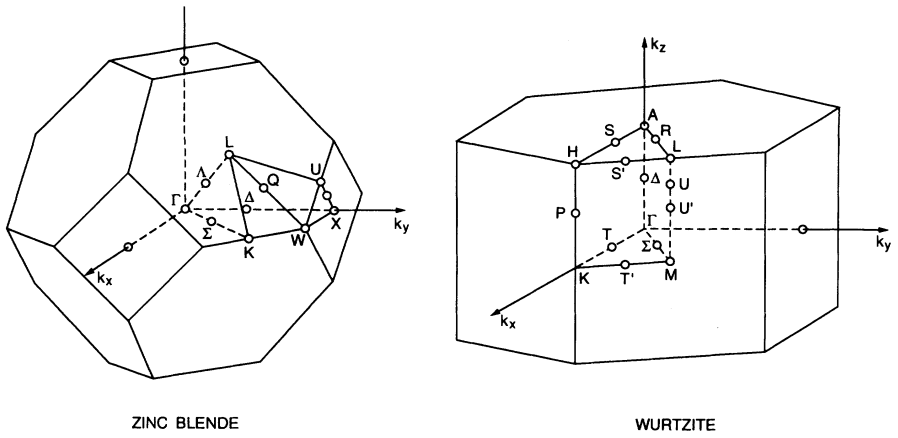

FIG. 7. Brillouin zones of the wurtzite and zinc-blende lattices.

$\frac{1}{3}\Gamma K$ (6→10) transitions. We relate peaks at 6.78 and 7.47 eV to small structures in the pseudopotential spectrum assigned also to transitions at the M and K points. The highest peak, split into two components at 8.0 and 8.2 eV, corresponds in energy (and in intensity) to the pseudopotential-spectrum peak at 8.1 eV, but the assignments are quite different. In our calculation the origin is not (around) the Γ point, but rather in the vicinity of the S and K points. We assume the corresponding peak in the experimental spectrum is either the one at 7.8 eV or the peak at 8.8 eV. The peak around 8.9 eV seems to correspond to the pseudopotential-spectrum peak at 9.2 eV (see Fig. 4 of Ref. 49), and maybe to the experimental one at 8.8 eV. At higher photon energies the

TABLE VIII. Peak positions (in eV) and the calculated origins of major contributions to structure in $\varepsilon_2(\omega)$ for InN.

Energy of optical structure (eV)			Major contribution transitions	
Experiment[a]	Calculations[b]	Our results	Transition	Energy (eV)
		3.17	A: 5 → 9; 8 → 10	3.13
4.0	4	3.75	Γ: 4, 5 → 10	3.78
		4.47	region around Δ: 5 → 10	4.48
5.0	4.8, 5.1	4.61, 4.73	$\frac{1}{3}\Gamma\Sigma$, $\frac{1}{6}\Gamma K$: 4 → 10	4.67, 4.87
		5.26	$\frac{2}{3}\Delta P$: 8 → 9	5.28
		5.63	$\frac{1}{3}\Gamma T'$: 6 → 10	5.53
	5.6	5.85	$\frac{1}{3}\Gamma K$: 6 → 10	5.84
	6.5	6.78	$M, \Gamma M$: 6 → 10	6.66–6.80
	7.35	7.47	K: 8 → 9	7.43
			$\frac{3}{4}TS$: 7 → 11	7.99
7.8	8.1	8.00, 8.20	$\frac{5}{6}\Gamma K$: 6 → 9	8.17
			$\frac{1}{3}\Delta P, TS$: 6 → 12	8.96, 8.85–8.89
8.8	9.2	8.90, 9.02		
			$\frac{2}{3}\Gamma M$: 5 → 10	9.09
			Δ: 8 → 12	9.30
		9.31	$\frac{2}{3}\Gamma K$: 6 → 11	9.33
			$\frac{1}{2}\Gamma K$: 7 → 13	9.33
		9.71	$\frac{1}{6}\Gamma K$: 6 → 12	9.68
		9.92	$\frac{1}{3}\Gamma\Sigma$: 6 → 12	9.92
		10.20	T: 8 → 14	10.22
		10.33	$\frac{1}{6}\Delta P$: 8 → 15	10.38
		10.45	A: 6 → 14	10.50–10.54
		10.69	$\Gamma, \Gamma A$: 4, 5 → 12, 13; 7, 8 → 15, 16	10.61–10.64
		11.14	Γ: 6, 7 → 15, 16	11.15
		11.55	$\frac{1}{3}\Gamma M$: 6 → 14	11.57

[a]Reflectance on single crystalline samples (Ref. 48).
[b]Empirical pseudopotential (Ref. 49).

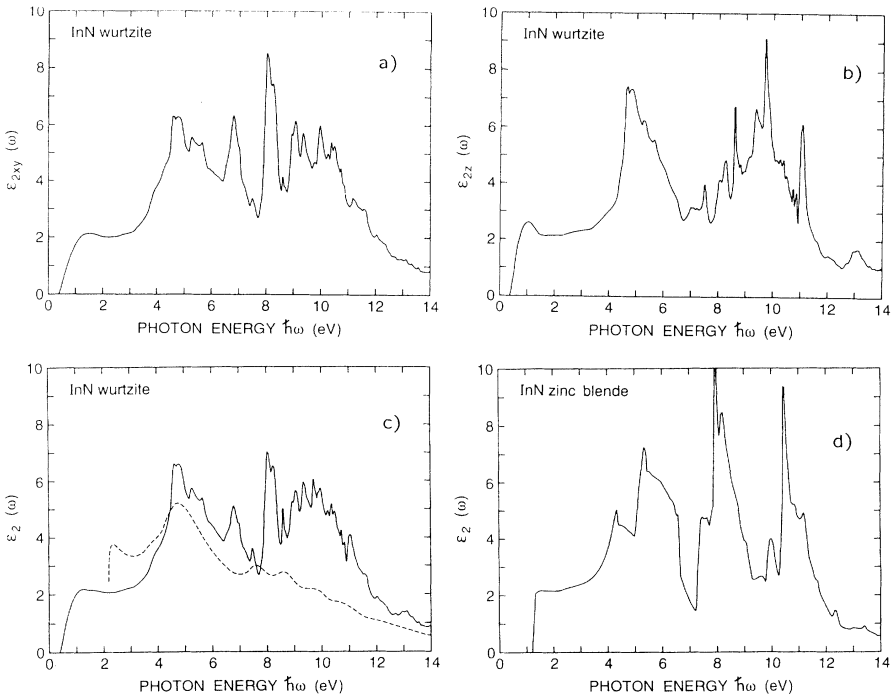

FIG. 8. Imaginary part of the dielectric function of InN. (a) Wurtzite structure, polarization in the xy plane; (b) wurtzite structure, polarization along the z axis; (c) wurtzite structure, average value over the three Cartesian directions; the solid line indicates our calculated result, and the broken line corresponds to experiment (Ref. 48); (d) zinc-blende structure.

analysis becomes more complicated. There is a series of peaks between 9.3 and 11.55 eV. Structures around 9.5, 10, and 11 eV are seen in the pseudopotential spectrum also (see Fig. 4 of Ref. 49), but there is no clear evidence for them in the experimental spectrum.

B. GaN and AlN

To our knowledge there are no experimental data concerning the dielectric function of GaN and AlN. In Figs. 9 and 10 we present our calculated imaginary parts of the dielectric function and in Tables IX and X our suggested assignment of structures in $\varepsilon_2(\omega)$ peak positions is given. The GaN and AlN spectra have some features in common. There are three groups of peaks. The first group is in the 6–9 eV photon energy range, and in GaN they are mainly due to transitions in the vicinity of M, but there are also contributions from the U, S', Σ, H, and K points. Similarly, the main peak in the dielectric function spectrum of AlN, situated at 8.08 eV, comes from

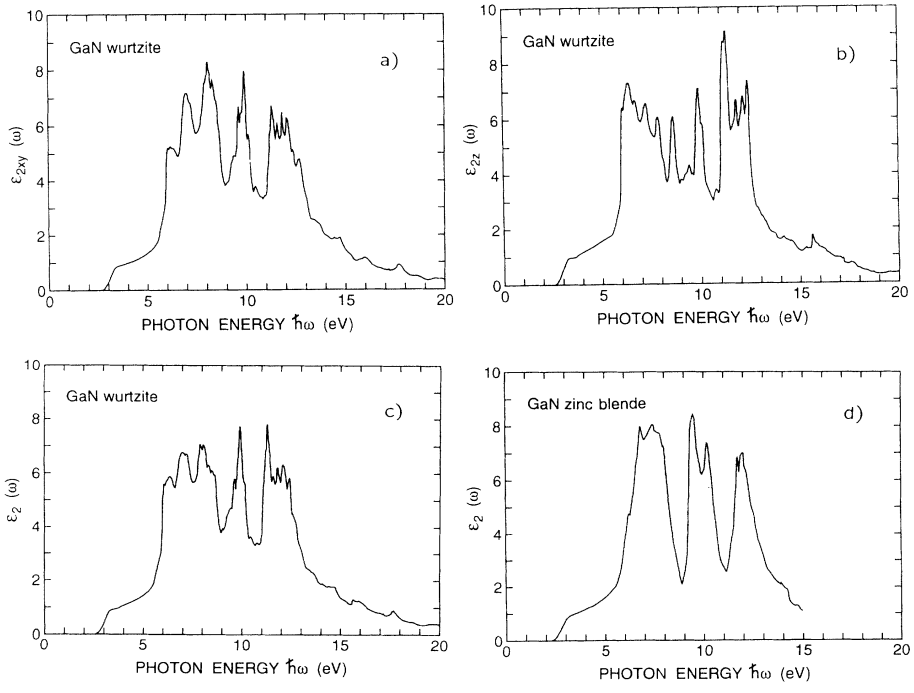

FIG. 9. Imaginary part of the dielectric function of GaN. (a) Wurtzite structure, polarization in the xy plane, (b) wurtzite structure, polarization along the z axis; (c) wurtzite structure, average value over the three Cartesian directions; (d) zinc-blende structure.

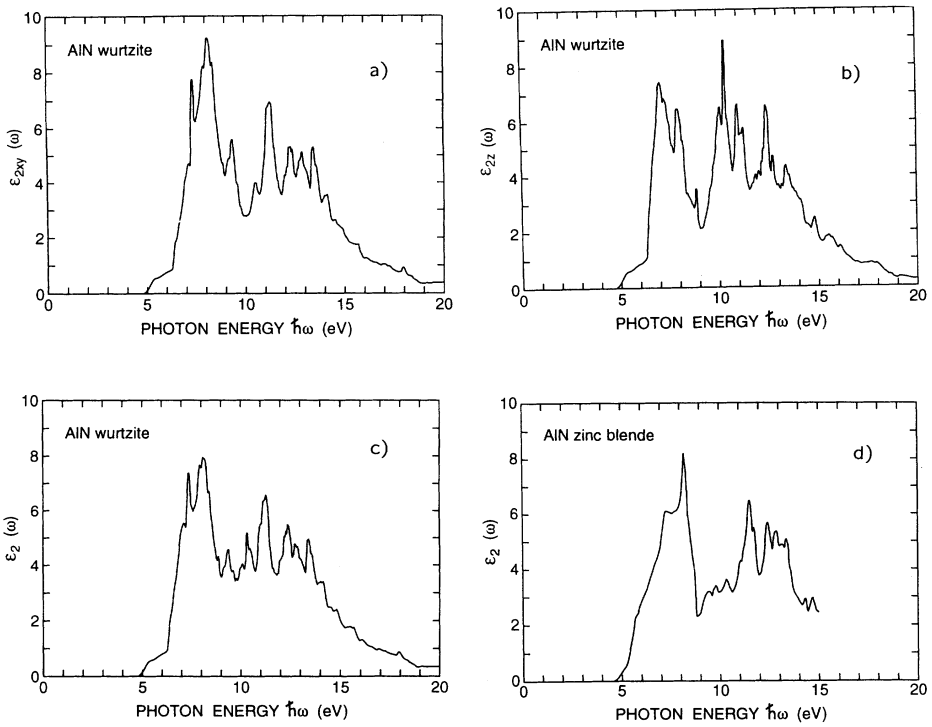

FIG. 10. Imaginary part of the dielectric function of AlN. (a) Wurtzite structure, polarization in the xy plane; (b) wurtzite structure, polarization along the z axis; (c) wurtzite structure, average value over the three Cartesian directions; (d) zinc-blende structure.

transitions at the M point. The second group of peaks (9–11 eV in GaN and 9–12 eV in AlN) is connected in GaN with transitions at P and L', whereas in AlN transitions in the vicinity of Σ, P, and L give the major contributions. The last group of peaks (up to 13.5 eV) comes mainly from transitions at Γ, A, and M (GaN) and T, M, and A (AlN) points of the Brillouin zone (BZ). Three similar groups of peaks are more clearly seen in the spectra for the zinc-blende structure.

C. BN

Our results for cubic BN are compared with experimental data obtained by Osaka *et al.*[51] from the reflectance spectrum by Kramers-Kronig transformation, and to the other theoretical results.[52,53] As is seen from Fig. 11(d) there is a very good overall agreement between the two curves considering their shape, and it appears easy to identify corresponding peaks. But it is seen that all the calculated peak positions are shifted towards *higher* photon energies. This is very surprising since LDA calculations generally understimate the band gaps, so we would have expected a shift in the opposite direction. A spectrum very similar to ours was obtained by Xu and Ching[53] using an orthogonalized linear combination of atomic orbitals (OLCAO) method. Their $\varepsilon_2(\omega)$ spectrum is also shifted towards higher energies when compared to experiment. Their calculations on large-gap insulators indicate that the major peaks in the optical absorption curves are in good agreement with experiments, even though the calculated main energy gaps are smaller than those measured (Ref. 53 and references therein). Detailed comparison of our calculated $\varepsilon_2(\omega)$ with experiment and other calculations [empirical pseudopotential[52] and OLCAO (Ref. 53)] is given in Table XI. The spectral positions of the peaks in our spectra agree well in general with other calculations, but our assignment to contributing interband transitions is entirely different from the one proposed in Ref. 52. The onset energy of absorption in our $\varepsilon_2(\omega)$ agrees with the value of the direct gap at the Γ point. Small structures appearing at energies 9.9–10.48 eV associated with 4→5 transitions at the Δ and Σ' points, and also containing 3→5 transitions close to $\frac{1}{2}\Gamma - U'$, seem to correspond to the experimental peak at 8.9 eV.The main peak consists of two components (11.97

TABLE IX. Peak positions (in eV) and the calculated origins of major contributions to structure in $\varepsilon_2(\omega)$ for GaN.

Energy of optical structure (eV)	Major contribution transitions	
	Transition	Energy (eV)
5.57	Γ: $4,5 \rightarrow 10$	5.55, 5.59
6.04	U: $8 \rightarrow 9$	5.92
6.33	$\frac{1}{4}ML$: $8 \rightarrow 10$	6.36
6.96	M: $8 \rightarrow 10$	6.90
7.30	S': $7,8 \rightarrow 9,10$	7.29
7.88	$M, \frac{1}{4}ML$: $6 \rightarrow 9$	7.86, 7.94
8.23	Σ: $6 \rightarrow 10$, H: $8 \rightarrow 9$	8.22, 8.26
8.51	K: $6 \rightarrow 9$	8.63
9.61	P: $7 \rightarrow 11$	9.79
9.88	L: $8 \rightarrow 11$	9.86
11.27	$\frac{1}{3}\Gamma M$: $7 \rightarrow 13$	11.27
11.55	$\frac{1}{6}AH$: $8 \rightarrow 13$	11.55
11.78	Γ: $5 \rightarrow 13$; $8 \rightarrow 14$	11.67, 11.66
12.08	M: $8 \rightarrow 13$	12.08
12.37	$\frac{1}{4}\Gamma A$: $8 \rightarrow 15$	12.38

TABLE X. Peak positions (in eV) and the calculated origins of major contributions to structure in $\varepsilon_2(\omega)$ for AlN.

Energy of optical structure (eV)	Major contribution transitions	
	Transition	Energy (eV)
6.35	$\frac{3}{4}\Gamma A$: $8 \rightarrow 9$	6.42
6.50	$\frac{3}{4}ML$: $8 \rightarrow 9$	6.56
7.10	$\frac{5}{6}AL$: $7,8 \rightarrow 9,10$	7.15
7.92	R : $7,8 \rightarrow 9,10, U'$: $6 \rightarrow 10$	7.86, 7.89
8.08	M : $6 \rightarrow 10$	8.05
8.37	vicinity of U' and M : $6 \rightarrow 10$	8.35, 8.37
9.35	$\frac{1}{4}\Sigma R$: $6 \rightarrow 10$	9.35
10.08	region around P: $8 \rightarrow 11$	10.05–10.11
11.27	region around L: $6,7 \rightarrow 12,13$	11.22–11.27
12.20, 12.29, 12.37	$T, M, 5/6\Gamma M$: $8 \rightarrow 13$	12.24, 12.26, 12.36
12.74	A: $5,6 \rightarrow 13,14$; $7,8 \rightarrow 15,16$	12.74
12.86	T: $7 \rightarrow 14$	12.80
13.43	Δ: $7,8 \rightarrow 15,16$	13.45

and 12.25 eV) and is assigned to transitions from band 4 to 5 at Σ and L points of the BZ. The experimental value is 11.0 eV, whereas other calculated transition energies are (much) higher. A shoulderlike structure in the experimental spectrum near 12.5 eV can be compared with the small peak at 12.79 eV assigned to transitions from band 4 to band 6 in a region close to L. The last peak in the experimental spectrum is situated at higher energy (16.4 eV) than the one calculated (14.8, 15.24 eV). It has main contributions from Δ and Σ' (4→6) transitions.

D. Static dielectric constants

In Table XII, the values of the dielectric constants $\varepsilon(0)$ and the pressure coefficients of refractive index, $1/n(dn/dP)$, are given in comparison with results of other calculations and experiments. In addition, Fig. 12 shows the pressure dependence of $\varepsilon(0)$. For all compounds considered we have got negative values of $1/n(dn/dP)$. Our results do not confirm the earlier predictions[57] that $1/n(dn/dP)$ is negative for III-V compounds, positive for II-VI, and nearly 0 for GaN (-0.05×10^{-2} GPa^{-1}). Our value for GaN is -0.19×10^{-2}GPa^{-1} and this is in very good agreement with experiment[39] (-0.2×10^{-2} GPa^{-1}). Incidentally, all experiments known to us measuring dn/dP of tetrahedrally coordinated semiconductors yield negative values. The calculated values of $\varepsilon(0)$ agree rather well with experiments, but they are systematically somewhat smaller. Comparing our values with those calculated by the OLCAO method[14] we see that they have found substantially

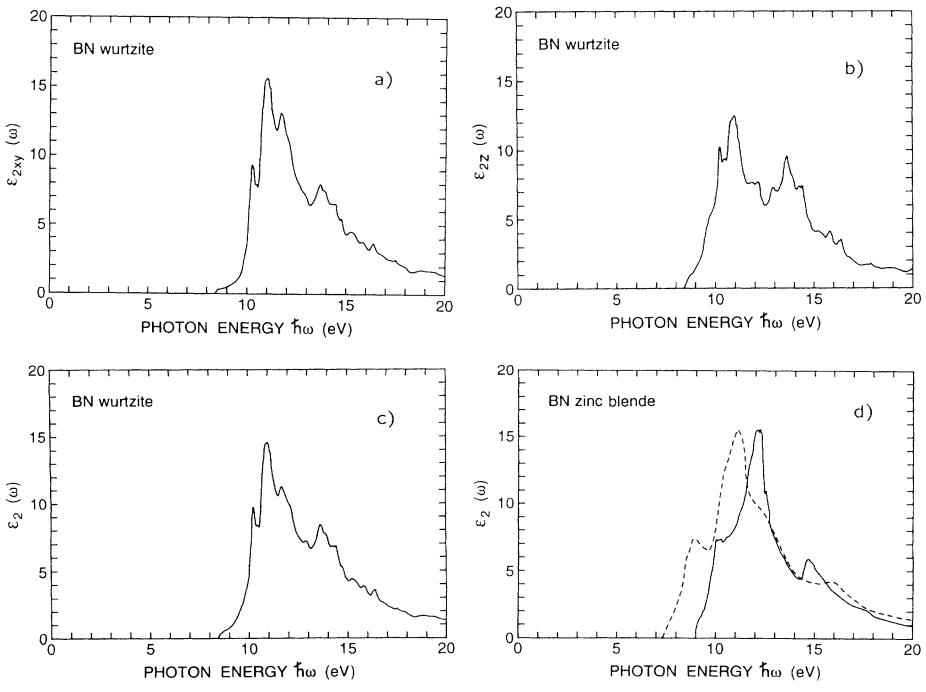

FIG. 11. Imaginary part of the dielectric function of BN. (a) Wurtzite structure, polarization in the xy plane; (b) wurtzite structure, polarization along the z axis; (c) wurtzite structure, average value over the three Cartesian directions; (d) zinc-blende structure; the solid line indicates our calculated result, the broken line corresponds to experiment (Ref. 51).

TABLE XI. Peak positions (in eV) and the calculated origins of major contributions to structure in $\varepsilon_2(\omega)$ for BN.

Energy of optical structure (eV)			Major contribution transitions	
Experiment[a]	Calculations	Our results	Transition	Energy (eV)
	8.4[b]	8.92	Γ: $4 \rightarrow 5$	8.92
	10.1[b]	9.35	X: $4 \rightarrow 5$	9.34
		9.90, 10.20	Δ, Σ':$4 \rightarrow 5$	9.88, 10.10
8.8	10.8,[b] 10.7[c]	10.48	$\frac{1}{2}\Gamma U$: $3 \rightarrow 5$	10.56
	12.7[b]	11.21	U: $4 \rightarrow 5$	11.20
11.0	13.5,[b] 12.6[c]	11.97, 12.25	Σ, L: $4 \rightarrow 5$	11.82, 12.20
12.5	13.8[b]	12.79	L: $4 \rightarrow 6$	12.53
16.4	15.1,[b] 15.6[c]	14.8, 15.24	Δ, Σ': $4 \rightarrow 6$	14.75, 16.20

[a]From reflectance spectrum by Kramers-Kronig transformation (Ref. 51).
[b]Empirical pseudopotential (Ref. 52).
[c]OLCAO (Ref. 53).

TABLE XII. The calculated electronic dielectric constants $\varepsilon(0)$ and the pressure coefficients of refractive index, $1/n(dn/dp)$ in units of 10^{-2} GPa^{-2}, for the nitrides in the wurtzite and zinc-blende structures. For the wurtzite structure the components of $\varepsilon(0)$ are given in the notation $\varepsilon = (\varepsilon_x + \varepsilon_y + \varepsilon_z)/3$, $\varepsilon_\perp = (\varepsilon_x + \varepsilon_y)/2$, $\varepsilon_\parallel = \varepsilon_z$. "Other results" includes experiments as well as theory.

	Wurtzite			Zinc-blende	
	Present work	Calculations[a]	Experiment	Present work	Other results
InN					
ε	7.16	7.390	8.4[b]	6.15	
$\varepsilon_\perp$	7.27	8.061			
$\varepsilon_\parallel$	6.94	7.054			
$1/n(dn/dp)$	-0.43			-0.39	
GaN					
ε	4.68	9.530	5.2,[c] 5.7[d]	4.78	
$\varepsilon_\perp$	4.71	11.159			
$\varepsilon_\parallel$	4.62	8.716			
$1/n(dn/dp)$	-0.19		-0.2[d]	-0.20	
AlN					
ε	3.86	4.272	4.68[e]	3.90	
$\varepsilon_\perp$	3.91	5.063			
$\varepsilon_\parallel$	3.77	3.876			
$1/n(dn/dp)$	-0.18			-0.18	
BN					
ε	4.14	4.065, 4.17[f]		4.14	3.86,[f] 4.5[g]
$\varepsilon_\perp$	4.19	4.232, 4.16[f]			
$\varepsilon_\parallel$	4.06	3.982, 4.18[f]			
$1/n(dn/dp)$	-0.06			-0.06	

[a]OLCAO (Ref. 14).
[b]From refractive index (Ref. 54).
[c]From refractive index (transmission and reflection) (Ref. 55).
[d]From refractive index (interference method) (Ref. 39).
[e]Infrared reflectivity at 300 K (Ref. 56).
[f]OLCAO (Ref. 53).
[g]Reference 9.

larger differences between ε_{xy} and ε_z (higher degree of anisotropy). The value given in Ref. 14 for the dielectric constant of GaN (9.53) is surprisingly large. Our value is 4.68, and reported experimental values are between 5 and 6.[39,55]

IV. PRESSURE-INDUCED STRUCTURAL PHASE TRANSITIONS

Certain rules derived from observed trends[1] connected with pressure-induced structural transformations in semiconductors show that less ionic III-V compounds transform into the β-tin structure, whereas more ionic III-V's and all II-VI compounds favor the rocksalt structure ($B1$) at moderate pressures and then, at higher pressures, change to other structures, e.g., β-Sn. In view of their high ionicities the nitrides are expected to transform to the rocksalt structure when pressure is applied.

In our total-energy calculations we examine several candidates for the high-pressure structures, rocksalt, β-Sn, and CsCl ($B2$). We also performed calculations for the zinc-blende structure ($B3$) which is very close in energy to the wurtzite structure. The details concerning the calculations for these structures are given elsewhere.[5] For each structure we calculated the total energy as a function of volume. The results are summarized in Figs. 13(a)–13(d) for GaN, AlN, InN, and BN, respectively. From the energy-volume relations for the given phase we derived the $T=0$ isotherm, the equilibrium volume, the bulk modulus, and the enthalpy vs pressure. The phase transition I→II occurs at the pressure at which the enthalpy of phase I equals that of phase II. As is seen from Fig. 13, the phase transitions for all the nitrides occur from the wurtzite (for BN from the zinc-blende) to the rocksalt structure. In Table XIII calculated equilibrium lattice constants, bulk moduli, and their pressure coefficients are listed for nitrides in wurtzite, zinc-blende, and rocksalt phases. Results of the calculated[62] phase transition parameters are given in Table XIV in compar-

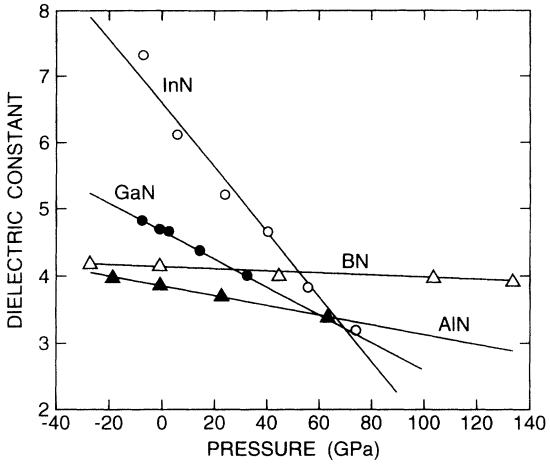

FIG. 12. Pressure dependence of $\varepsilon(0)$ for the III-V nitrides in the wurtzite structure. The calculated points are indicated (open circles, InN; filled circles, GaN; filled triangles, AlN; and open triangles, BN). The lines represent least-squares fits to the calculations.

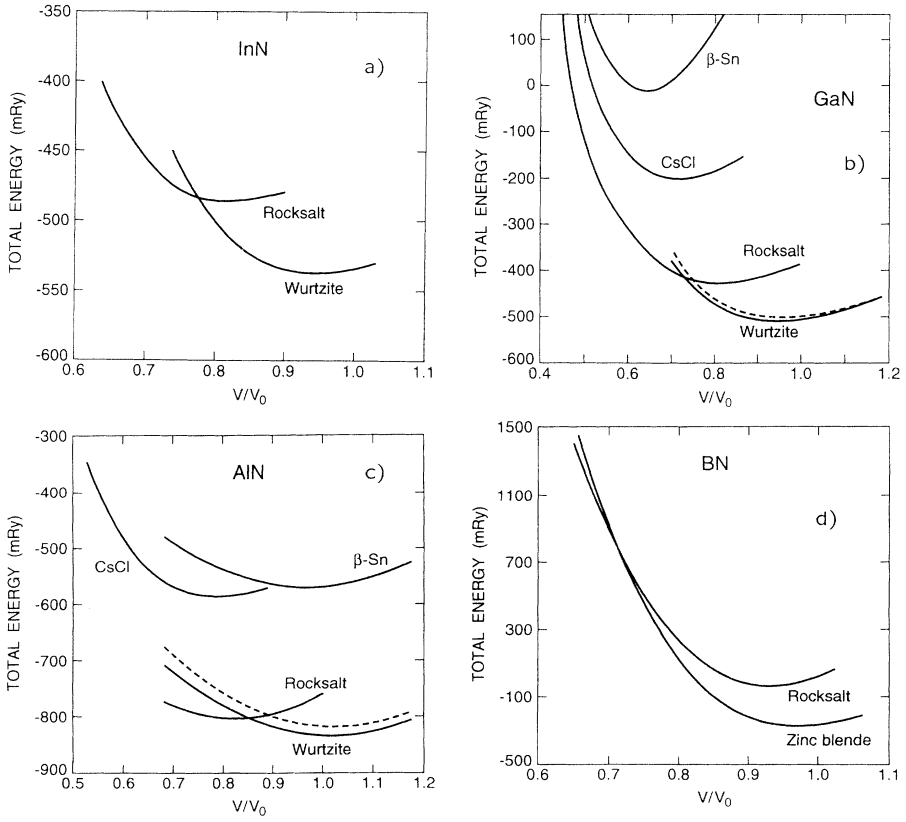

FIG. 13. Calculated total energies of InN (a), GaN (b), AlN (c), and BN (d) in different crystollographic structures as a function of volume relative to the experimental equilibrium volume. Dashed curves in (b) and (c) correspond to the zinc-blende structure.

ison with other theoretical results as well as experimental data. (Reference 62 uses some LMTO-specific concepts which are all explained in Andersen's original paper.[2])

It follows from Table XIV that the phase transition pressure varies considerably from one compound to another. It is about three times higher for GaN than for AlN, and extremely high for BN. It is surprising that GaN and AlN, having very similar bond lengths, ionicity, and bulk modulus, differ so much regarding their structural phase transition. The phase transition of GaN is located at about 50 GPa whereas in AlN we observed the transition at a considerably lower pressure—about 16 GPa. It was suggested by Chelikowsky[64] that the transition pressure from the tetrahedrally coordinated structure (wurtzite, zinc-blende) to the rocksalt structure changes linearly with Phillips ionicity for the same atomic volume. Our results do not agree with this prediction (see Table VII). The situation seems better when we use the ionicity scale postulated by Vogl and Majewski,[65] based on the atomic terms of anions and cations. We can see that, in contrast to the Phillips scale, GaN and AlN differ importantly in their ionicities, which is reflected in their structural stability. It was suggested by Froyen and Cohen[66] that of two compounds of similar ionicity the

TABLE XIII. The calculated equilibrium lattice constants a, bulk moduli B, and the pressure derivatives of the bulk moduli B' for the nitrides in the wurtzite, zinc-blende, and rocksalt structures. The a given for the wurtzite structures are the "effective lattice constants" (cf. Table VII). For the rocksalt structure are also given (in parentheses) values corresponding to the volume to which the phase transition occurs. "Other results" includes experiment and theory.

	Wurtzite			Zinc blende		Rocksalt	
	Present work	Other calc.	Expt.	Present work	Other results	Present work	Other results
InN							
a (Å)	4.922		4.98[a]	4.95		4.65(4.49)	
B (GPa)	125	166,[b]212[c]	125.5[d]	137		154(251)	
B'	8.1	3.40[c]	12.7[d]	4.3		8.8	
GaN							
a (Å)	4.433		4.50[a]	4.46	4.419,[b]4.54[j]	4.18(3.96)	4.098[b] 4.22[e]
B (GPa)	200	190,[b] 203,[c]179,[e] 176,[f]240[g]	237,[d] 245,[h] 195[i]	184	173[b]	227(397)	223[b]
B'	3.8	2.92,[b] 3.98[c] 3.93,[e]2.66[f]	4.3[d]	4.6	3.64[b]	4.0	3.69[b]
AlN							
a (Å)	4.357		4.37[a]	4.37		4.06(3.99)	4.032[b]
B (GPa)	220	195,[b]207,[c,k] 205[l]	207.9[m]	215	216[l]	281(348)	270[l]
B'	3.9	3.74,[b]5.60[c] 3.98[k]	6.3[m]	4.0		4.0	
BN							
a (Å)	3.619			3.62	3.615[a] 3.768[n] 3.606[o]	3.50(2.82)	3.493[o]
B (GPa)	391	392[c]	390[d]	378	375,[n]367[o]	406(2750)	425[o]
B'	3.7	6.38[c]	3.5[d]	3.4		3.7	

[a]Reference 9.
[b]Nonlocal pseudopotential (Ref. 18).
[c]OLCAO (Ref. 14).
[d]X-ray diffraction (Ref. 58).
[e]Norm conserving pseudopotential (Ref. 35).
[f]Norm conserving pseudopotential (Ref. 19).
[g]Norm conserving pseudopotential (Ref. 20).
[h]Extended x-ray fine structure (EXAFS) (Ref. 23).
[i]From values of atomic displacements (Ref. 59).
[j]Transmission electron microscopy (Ref. 60).
[k]LCAO (Ref. 24).
[l]Full-potential LMTO (Ref. 11).
[m]X-ray diffraction (Ref. 61).
[n]Pseudopotential with nonlocal exchange potential (Ref. 31).
[o]Nonlocal pseudopotential (Ref. 30).

TABLE XIV. The calculated structural phase transition (1→2) pressures P_c and relative volumes V_1/V_0 and V_2/V_0 of the two phases at the transition pressure. V_0 is the experimental equilibrium volume of phase 1 (wurtzite for InN, GaN, and AlN, and zinc blende for BN).

	Present work	Other calculations	Experiment
InN			
P_c (GPa)	21.6	5.0[a]	23.0,[b] 12.1[c]
V_1/V_0	0.85		
V_2/V_0	0.72		
GaN			
P_c (GPa)	51.8	55[a]	52.2,[c] 47–50[d]
V_1/V_0	0.81	0.82[a]	0.86[d]
V_2/V_0	0.69	0.71[a]	0.73[d]
AlN			
P_c (GPa)	16.6	12.9,[e] 12.5[f]	22.9,[c] 14–16.5[d]
V_1/V_0	0.93	0.95[e]	0.93,[d] 0.92[g]
V_2/V_0	0.76	0.77[e]	0.74[g]
BN			
P_c (GPa)	850	1 110[h]	
V_1/V_0	0.51	0.45[h]	
V_2/V_0	0.47	0.42[h]	

[a]Norm conserving pseudopotential (Ref. 35).
[b]Visual observation (Ref. 39).
[c]X-ray diffraction (Ref. 58).
[d]EXAFS (Ref. 23); visual observation (Ref. 39).
[e]Nonlocal pseudopotential (Ref. 18).
[f]Full-potential LMTO (Ref. 11).
[g]X-ray diffraction (Ref. 61).
[h]Nonlocal pseudopotential (Ref. 63).

one with the larger average gap (as is indeed the case for Al compounds) is the one that is more stable in the rocksalt structure. But differences in structural stability can also be related to the presence or absence of d-like states in the constituent atoms, as was shown by Sasaki *et al.*[67] As follows from the discussion in Sec. V, we can by means of the ASA pressure expressions demonstrate that this is indeed the case. Finally it is worth noting that the rocksalt phases, according to our calculations (even in LDA), are semiconducting for all the nitrides considered. This is interesting in view of the theory[66] predicting the metallic rocksalt phase for III-V compounds and a nonmetallic phase for II-VI compounds. Also, it follows from experiments[39] that the observed high pressure phases of GaN, AlN, and InN are nonmetallic.

V. DISCUSSION AND SUMMARY

It has been attempted here to give a rather comprehensive presentation of the results that we have obtained so far within the LDA for the III-V nitrides. When these are compared to experiments one should of course recall the known "deficiencies" of the LDA-eigenvalue spectrum. But it is also important to observe that most quantities are sensitive to structural data, especially to the volume. Some samples used in experiments are grown on lattice-mismatching substrates, and as a result the volume and strain state may not easily be specified. Such complications occur, for example, in the case of GaN in the zinc-blende form. The experimental data of wurtzite GaN are probably more reliable because in that case crystals of good quality can be produced without evaporation onto a substrate. Also, comparing different theoretical calculations it is essential that results for identical structures and volumes are compared. This seems obvious, but one should be aware, for example, that "equilibrium" in some cases is taken to mean "theoretical equilibrium" and in other "experimental equilibrium."

The electronic band structure, its pressure dependence, the dielectric functions, and pressure-induced structural phase transitions have been calculated. By comparing the pressure coefficients of the gaps in several semiconductors we find that trends in the dE_g/dP values cannot be established by considering them to depend only on the bond lengths. The ionicities must be included also in order to obtain a systematic description.

The total-energy calculations suggest that all the nitrides (InN, GaN, AlN, and BN) under pressure transform to the semiconducting rocksalt structure usually predicted as a high pressure phase of II-VI compounds. This result is a manifestation of the large ionicity of the nitrides. Using the LMTO method in a version that does not apply a downfolding technique,[68] we have seen that, in particular, the cases (GaN and InN) requiring calculations in two energy panels must be performed with a proper choice of linearization energies for the upper-panel cation d states. Improving this technical detail[62] gave structural transition pressures that differ from our earlier published values. Also we examined the effects on the calculated fundamental gaps in GaN and InN of including simultaneously coupling to the low-lying semicore d states and to the high-lying empty d states.

Surprisingly, the values of the phase transition pressure to the rocksalt structure are very different for the two otherwise quite similar compounds GaN and AlN. The transition pressure for GaN is three times that of AlN, and this may at first appear very peculiar since the ionicities (see Table VII) are quite similar. In fact, the ionicity of GaN may even be slightly *higher*[41,1] than that of AlN, and that would, according to observed trends, suggest that the transition pressure in GaN should be a bit lower than that of AlN. There have been suggestions that differences in cation orbital energies could explain the result, but such differences would manifest themselves in the ionicity values. According to our calculations (zinc-blende structure) the offsets between the sp^3 hybrid levels are 0.992 Ry and 0.948 Ry in GaN and AlN, respectively. These are the ionic gap components (the C's) in Phillips' complex gap. So neither these energies nor the ionicities would explain the fact that the transition pressure is (much) higher in GaN. There must therefore be a particular reason why the general trend is so far from being applicable to comparison between these two compounds. The puzzle is resolved by noting that Ga has d states in the (semi)core (the $3d$ states) and Al has not. For this reason the unoccupied d's ($4d$ in Ga and $3d$ in Al) lie much higher in Ga than in Al. Comparing calculations (taking the zinc-blende structure as

an example) at the same (compressed) volumes (atomic-sphere radius equal to 1.90 bohrs) we find that the center [the energy where the logarithmic derivative equals $-l-1$ (Ref. 2)] of the Ga $4d$ states lies 4.9 Ry above the N p center, whereas the separation between the Al $3d$ and N p band centers is 1.6 Ry lower in AlN. The square-well pseudopotentials (the V values[2]) of the cation d states exhibit similar trends, 0.3 Ry in GaN and -1.64 Ry in AlN. This means that the cation-d–anion-p hybridization is stronger in AlN than in GaN. Simultaneously it implies that the d partial pressures are very different in the two cases. The actual calculation shows that the d component of the pressure is rather large in magnitude and *negative* in AlN, whereas it is small and positive in GaN. These results can be understood from the energies above in terms of the discussion of the "tail pressures" in Ref. 69 [see in particular Eq. (30b) in that paper: the prefactor has opposite signs in GaN and AlN]. This explains why the equilibrium volume of AlN is smaller than that of GaN, a result that would also be expected by stating that the Ga atom is "larger" than Al. But we can understand from our detailed analysis that this hybridization effect will increase under pressure, i.e., the difference in strength between the d bonding in AlN and GaN becomes more pronounced when the volumes are reduced. As a consequence the *ratio* between the zero-pressure volume in the rocksalt phase and the equilibrium volume of the wurtzite phase, $V_0(B1)/V_0(\mathrm{wur})$, is smaller in AlN than in GaN. Our actual calculations (Table XIII) show that this ratio is 0.809 for AlN and 0.838 for GaN, i.e., the ordering just anticipated. In view of this, we can then also understand that the slope, disregarding sign, of the common tangent to the rocksalt and wurtzite total-energy curves, when energies are plotted as functions of V/V_0, is *lower* for AlN than for GaN. Thus, AlN must have the lower transition pressure.

Most calculations of the wurtzite phases were performed here by assuming that c/a and u have their ideal values. It is realized, however, that a full structural relaxation can change some of the gaps by 0.05–0.2 eV. In AlN the relaxation reduces the direct gap at Γ by 0.21 eV, in InN by 0.06 eV, and in GaN by only 0.05 eV. This has some relevance to the discussion of differences between gaps in the wurtzite and zinc-blende nitride phases.

For GaN we made an estimate of the "LDA gap error" using the Bechstedt–Del Sole approximation.[70] This correction is 1.3 eV. Recent *GW* calculations for zinc-blende GaN show[29] that the correction to the fundamental gap is 0.88 eV (experimental equilibrium volume) and 0.97 eV at the theoretical equilibrium volume. Using our best LDA gaps (including structural relaxations) together with these *GW* calculations gives, if we take the values at the experimental volume, $E_g \approx 3.0$ (cubic) to 3.2 eV (hexagonal). These seem to be too low by ≈ 0.2–0.4 eV when compared to experiments.

The optical spectra were derived from the LDA one-electron band structures, but nevertheless we find static dielectric constants which are (slightly) smaller than the experimental values. This may appear somewhat surprising since local-field effects, not included here, tend to lower the values of $\varepsilon(0)$.[43–45] But, as pointed out previously, the accuracy of our calculated amplitudes is affected by the use of the atomic-sphere approximation. The intensities are influenced by how space is divided up into "anion spheres" and "cation spheres". Corrections, in line with the calculation of "combined corrections,"[2] can be made. In addition the way of treating semicore d states also affects the $\varepsilon(0)$ values. Lambrecht[71] has recently examined this for zinc-blende-type GaN, where he finds that including the Ga $3d$'s in the basis instead of the $4d$ states (and using the same potential) increases ε by 0.3. Although the dielectric functions which we have presented here are derived from the LDA eigenvalues and transition matrix elements, we believe that the analyses identifying the origins of various elements of structure in the spectra are useful for the interpretation of optical experiments. To our surprise we found that for BN the $\varepsilon_2(\omega)$ spectrum calculated within the LDA seems to be upshifted in energy when compared to experiment. We are not, at the present, able to produce spectra based on band structures where adjusting potentials have been included. In spite of the increasing amount of experimental data on the properties of the III-V nitrides, the measurements of major gaps are still not sufficiently detailed to allow the determination of the parameters of such external potentials. A rigid shift of the conduction bands relative to the valence bands does not yield the correct dispersion. Also, for this very reason, we have not attempted to calculate effective masses at the band-edge extrema.

ACKNOWLEDGMENTS

We thank L. Reining for discussions of gap corrections and for communicating the results of the *GW* calculations[29] prior to publication. Also discussions and exchange of unpublished results with W. Lambrecht and B. Segall have been very fruitful. One of us (I.G.) would like to acknowledge the financial support from the Polish Committee of Scientific Research (Grant No. 30068 91 01) as well as the Danish Rector's Conference (Grant No. 1993-9328-2). The project was further supported by Grant No. 11-9001-3 from the Danish Natural Science Research Council, and we have benefited from support from Hewlett-Packard.

[1] J.A. Van Vechten, Phys. Rev. **182**, 891 (1969); **187**, 1007 (1969).
[2] O.K. Andersen, Phys. Rev. B **12**, 3060 (1975).
[3] N.E Christensen, Phys. Rev. B **30**, 5753 (1984); M. Cardona, N.E. Christensen, and G. Fasol, *ibid.* **38**, 1806 (1988).
[4] N.E. Christensen and O.B. Christensen, Phys. Rev. B **33**, 4739 (1986).
[5] I. Gorczyca and N.E. Christensen, Solid State Commun. **80**, 335 (1991).
[6] G.B. Bachelet and N.E. Christensen, Phys. Rev. B **31**, 879

(1985).
[7]N.E. Christensen, Phys. Rev. B **37**, 4528 (1988).
[8]N.E. Christensen and M. Methfessel, Phys. Rev. B **48**, 5797 (1993).
[9]*Numerical Data and Functional Relationships in Science and Technology*, edited by O. Madelung, M. Schulz, and H. Weiss, Landolt-Börnstein, New Series, Vol. 17a (Springer-Verlag, Berlin, 1982).
[10]H. Schultz and K.H. Thiemann, Solid State Commun. **23**, 813 (1977).
[11]N.E. Christensen and I. Gorczyca, Phys. Rev. B **47**, 4307 (1993).
[12]C.-Y. Yeh, Z.W. Lu, S. Froyen, and A. Zunger, Phys. Rev. B **46**, 10 086 (1992).
[13]S.N. Grinyaev, V.Ya. Malakhov, and V.A. Chaldyshev, Izv. Vyssh. Uchebn. Zaved. Fiz. **4**, 69 (1986).
[14]Yong-Nian Xu and W.Y. Ching Phys. Rev. B **48**, 4335 (1993).
[15]W.R. Lambrecht and B. Segall (unpublished).
[16]R.B. Zetterstrom, J. Mater. Sci. **5**, 1102
[17]W.A. Tyagay *et al.*, Fiz. Tekh. Poluprovodn. **11**, 2142 (1977) [Sov. Phys. Semicond. **11**, 1257 (1977)].
[18]P.E. Van Camp, V.F. Van Doren, and J.T. Devreese (unpublished); Phys. Rev. B **44**, 9056 (1991); Solid State Commun. **81**, 23 (1992).
[19]M. Palumno, C.M. Bertoni, L. Reining, and F. Finochi, Physica B **185**, 404 (1993).
[20]B.J. Min, C.T. Chan, and K.M. Ho, Phys. Rev. B **45**, 1159 (1992).
[21]B. Monemar, Phys. Rev. B **10**, 676 (1974).
[22]S. Bloom, G. Harbeke, E. Meier, and I.B. Ortenburger, Phys. Status Solidi B **66**, 161 (1974).
[23]P. Perlin, C. Jauberthie-Carillon, J.P. Itie, A. San Miguel, I. Grzegory, and A. Polian, High Press. Res. **71**, 96 (1991); (unpublished).
[24]W.Y. Ching and B.N. Harmon, Phys. Rev. B **34**, 5305 (1986).
[25]B. Perry and R.F. Rutz, Appl. Phys. Lett. **33**, 319 (1978).
[26]V. Fiorentini, M. Methfessel, and M. Scheffler, Phys. Rev. B **48**, 13 353 (1993).
[27]S. Strite, J. Ruan, Z. Li, A. Salvador, H. Chen, D.J. Smith, W.J. Choyke, and H. Morkoç, J. Vac. Sci. Technol. B **9**, 192 (1991).
[28]T. Lei, T.D. Moustakas, R.J. Graham, Y. He, and S.J. Berkowitz, J. Appl. Phys. **71**, 4933 (1992).
[29]M. Palummo, L. Reining, R.W. Godby, C.M. Bertoni, and N. Börnsen (unpublished).
[30]R.M. Wentzcovitch, K.J. Chang, and M.L. Cohen, Phys. Rev. B **34**, 1071 (1986).
[31]K. Kikuchi, T. Uda, A. Sakuma, M. Hirao, and Y. Murayama, Solid State Commun. **81**, 653 (1992).
[32]V.A. Fomichev and M.A. Rumsh, J. Phys. Chem. Solids **29**, 1015 (1968).
[33]R.M. Chrenko, Solid State Commun. **14**, 511 (1974).
[34]N. Miyata and K. Moriki, Phys. Rev. B **40**, 12 028 (1989).
[35]A. Munoz and K. Kunc, Phys. Rev. B **44**, 10 372 (1991).
[36]U. Schmid, N.E. Christensen, and M. Cardona, Solid State Commun. **75**, 39 (1990).
[37]X. Zhu, S. Fahy, and S.G. Louie, Phys. Rev. B **39**, 7840 (1989).
[38]W. Hanke and L.J. Sham, Solid State Commun. **71**, 211 (1989).
[39]P. Perlin, I. Gorczyca, N.E. Christensen, I. Grzegory, H. Teisseyre, and T. Suski, Phys. Rev. B **45**, 13 307 (1992); P. Perlin, I. Gorczyca, S. Porowski, T. Suski, N.E. Christensen, and A. Polian, Jpn. J. Appl. Phys. **32**, 334 (1993).
[40]W. Paul, Prog. Semicond. **7**, 135 (1963).
[41]A. Garciá and M.L. Cohen, Phys. Rev. B **47**, 4215 (1993).
[42]N.E. Christensen, S. Sapathy, and Z. Pawlowska, Phys. Rev. B **36**, 1032 (1987).
[43]W. Hanke and L.J. Sham, Phys. Rev. Lett. **33**, 582 (1974).
[44]S.G. Louie, J.R. Chelikowsky, and M.L. Cohen, Phys. Rev. Lett. **34**, 155 (1975).
[45]M. Alouani, L. Brey, and N.E. Christensen, Phys. Rev. B **37**, 1167 (1988).
[46]M. Alouani, S. Gopalan, M. Garriga, and N.E. Christensen, Phys. Rev. Lett. **61**, 1643 (1988).
[47]I. Gorczyca, N.E. Christensen, and M. Alouani, Phys. Rev. B **39**, 7705 (1989).
[48]Q. Guo, O. Kato, M. Fujisawa, and A. Yoshida, Solid State Commun. **83**, 721 (1992).
[49]C.P. Foley and T.L. Tansley, Phys. Rev. B **33**, 1430 (1986).
[50]C. Wang and B.M. Klein, Phys. Rev. B **24**, 33 417 (1981).
[51]Y. Osaka, A. Chayahara, H. Yokoyama, M. Okamoto, T. Hamada, and M. Fujisawa, in *Synthesis and Properties of Boron Nitride*, edited by J.J. Pouch and S.A. Alteroviz (Trans Tech, Aedermannsdorf, Switzerland, 1990), pp. 227–292.
[52]L.A. Hemstreet, Jr. and C.Y. Fong, Phys. Rev. B **6**, 1464 (1972).
[53]Yong-Nian Xu and W.Y. Ching, Phys. Rev. B **44**, 7787 (1991).
[54]J. Misek and F. Srobar, Elektrotech. Cas. **30**, 690 (1979).
[55]E. Ejder, Phys. Status Solidi A **5**, 445 (1971).
[56]L. Akasaki and M. Hashimoto, Solid State Commun. **5**, 851 (1967).
[57]D.L. Camphausen, G.A. Neville Conell, and W. Paul, Phys. Rev. Lett. **26**, 184 (1971).
[58]M. Ueno, M. Yoshida, and A. Onodera (unpublished).
[59]A. Sheleg and V. Savastenko, Inorg. Mater. **15**, 1257 (1979).
[60]M. Paisley, Z. Sitar, J. Posthill, and R. Davis, J. Vac. Sci. Technol. A **7**, 701 (1989).
[61]M. Ueno, A. Onodera, O. Shimomura, and K. Takemura, Phys. Rev. B **45**, 10 123 (1992).
[62]Note that our results given here differ somewhat from the values of transition pressures that we have presented elsewhere. First of all, Table 2 of the paper in Physica B **185**, 410 (1993) contains misprints: P_c of InN and BN should be 23 GPa and 1025 GPa, respectively, and also the value, 11 100 GPa, cited from Ref. 32 of that paper is off by a factor of 10. Similar remarks apply to the P_c values, 254, 230, 10 250, and 11 100, given in Table III of Ref. 39 (pressures in kbars instead of GPa in these cases). In addition, our theoretical values in some cases have changed because we now use a much more dense mesh in **k** space than earlier (more than 400 points in the irreducible zone). This improves the accuracy of the Brillouin-zone integrations. Further, in the cases where the LMTO calculations need the use of two energy panels (GaN and InN), we have changed a technical detail concerning the choice of the linearization energy [E_ν in LMTO language (Ref. 2)] for the unoccupied d states (Ga $4d$ in GaN and In $5d$ in InN) in the upper panel. In order to avoid spurious bands this energy must be fixed at a level somewhat above the valence-band maximum. Previously we picked a value very high up, well inside the canonical d band (Ga $4d$, In $5d$, respectively) and used this same value at all volumes. Now we prefer, after a detailed study on other compounds also, rather to fix the value of the corre-

sponding logarithmic derivative $[D_\nu(d)]$. We choose a value, $D_\nu(d)=0.7$, such that $E_\nu(d)$ is located below the canonical d-band bottom $[D_\nu(d)=0]$, but above the square-well pseudopotential $[D_\nu=l,\ (l=2)]$. The corresponding $E_\nu(d)$ now varies with volume. The effect of this on the calculated transition pressure is not negligible. For GaN we now get $P_c=52$ GPa, whereas we earlier found 65 GPa. The correction to P_c is smaller in InN, 21.6 GPa instead of 25.4 GPa. With the new values we no longer have the discrepancy between theory and experiment which was particularly serious for GaN (experimental P_c of 47–50 GPa).

[63]R.M. Wentzcovitch and M.L. Cohen, Phys. Rev. B **36**, 6058 (1987).

[64]J.R. Chelikowsky, Phys. Rev. B **35**, 1174 (1987).

[65]P. Vogl and J.A. Majewski, in *Proceedings of the 19th International Conference on the Physics of Semiconductors, Warsaw, Poland, 1988*, edited by W. Zawadzki (Institute of Physics, Polish Academy of Sciences, Warsaw, 1988), p. 837.

[66]S. Froyen and M.L. Cohen, Solid State Commun. **43**, 447 (1982); Physica B&C **117B&118B**, 561 (1983).

[67]T. Sasaki, K. Shindo, K. Nizeki, and A. Morita, J. Phys. Soc. Jpn. **57**, 978 (1988).

[68]O.K. Andersen, O. Jepsen, and D. Glötzel, in *Highlights of Condensed-Matter Theory*, edited by F. Bassani, F. Fumi, and M.P. Tosi (North-Holland, New York, 1985).

[69]N.E. Christensen and V. Heine, Phys. Rev. B **32**, 6145 (1985).

[70]F. Bechstedt and R. Del Sole, Phys. Rev. B **38**, 7710 (1988).

[71]W.R.L. Lambrecht (private communication).